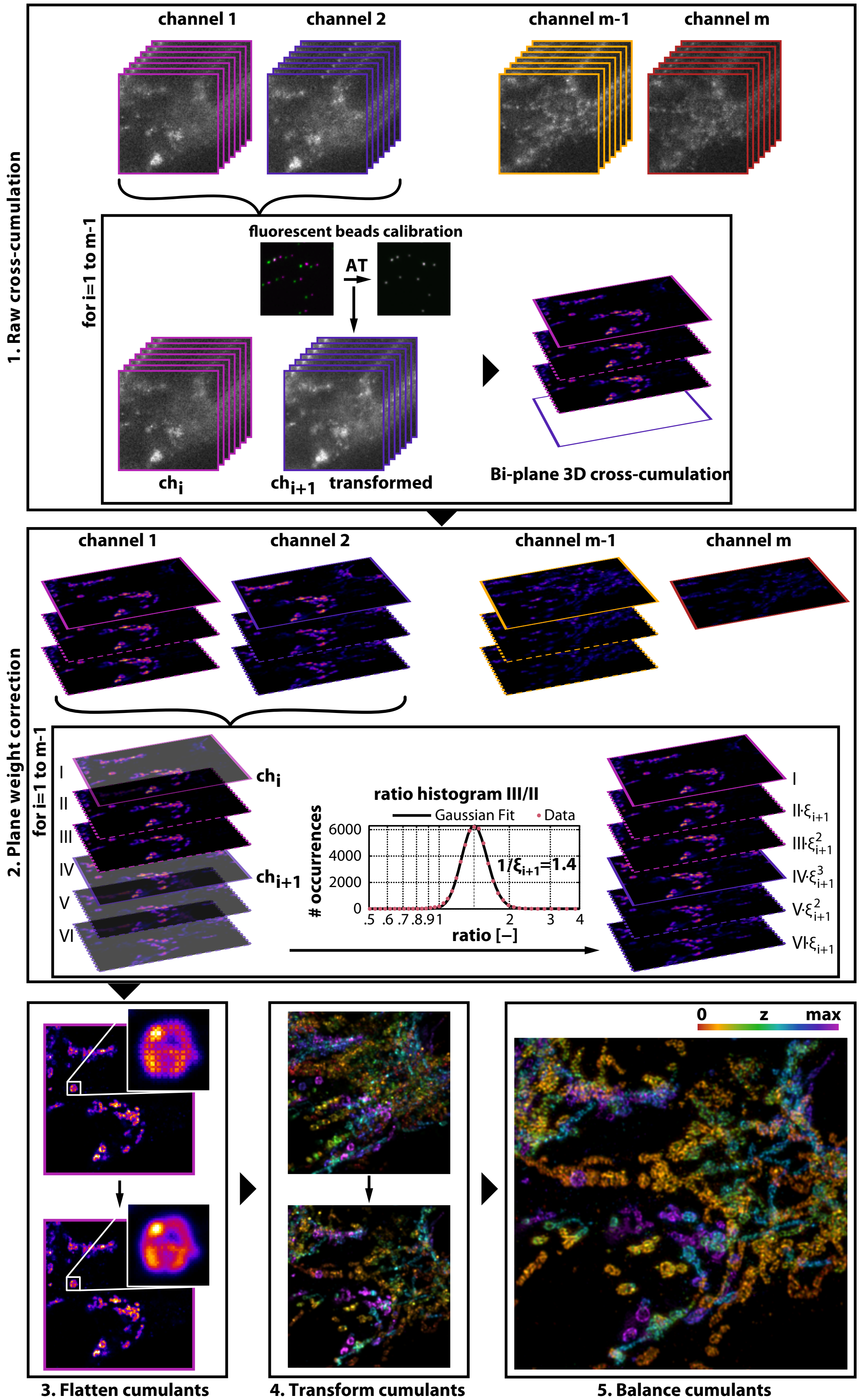

Supplementary Figure 1: Flowchart of the multiplane SOFI analysis exemplified for the third order.

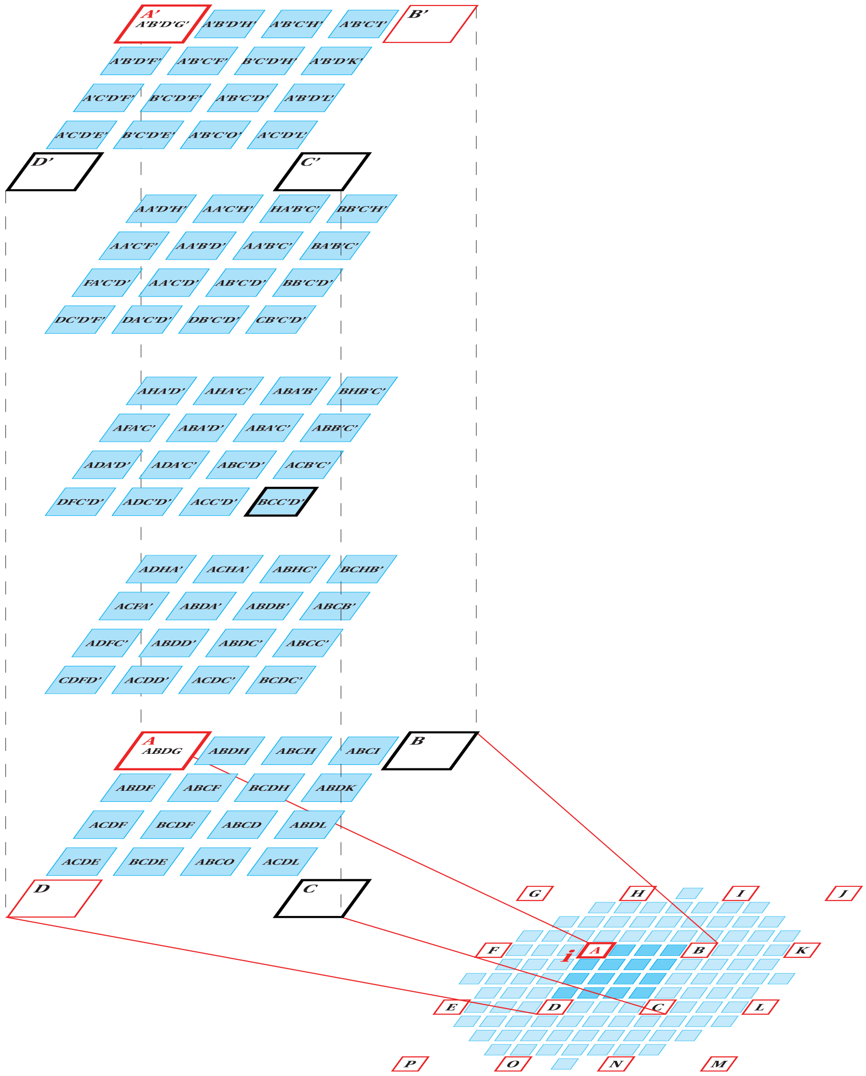

Supplementary Figure 2: Fourth order cross-cumulant combinations using multiplane detection. Each corresponding pixel pair $\mathbf{i}$ and $\mathbf{i}'$ can be complemented by 78 additional output pixels using different pixel combinations within a $4 \times 4 \times 2$ neighborhood. As an example, the pixel combination leading to the virtual pixel BCC’D’ has been highlighted with black borderlines.

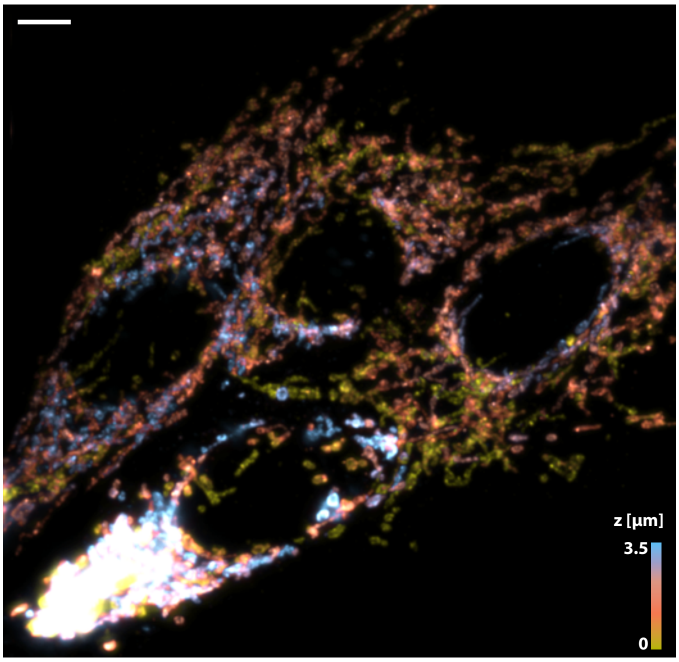

Supplementary Figure 3: Maximum intensity projection of the second-order SOFI image of mitochondria stained with Alexa 647 in fixed C2C12 cells (cf. third-order balanced SOFI image in Fig. 3.a). *Scale bar: 5 µm*

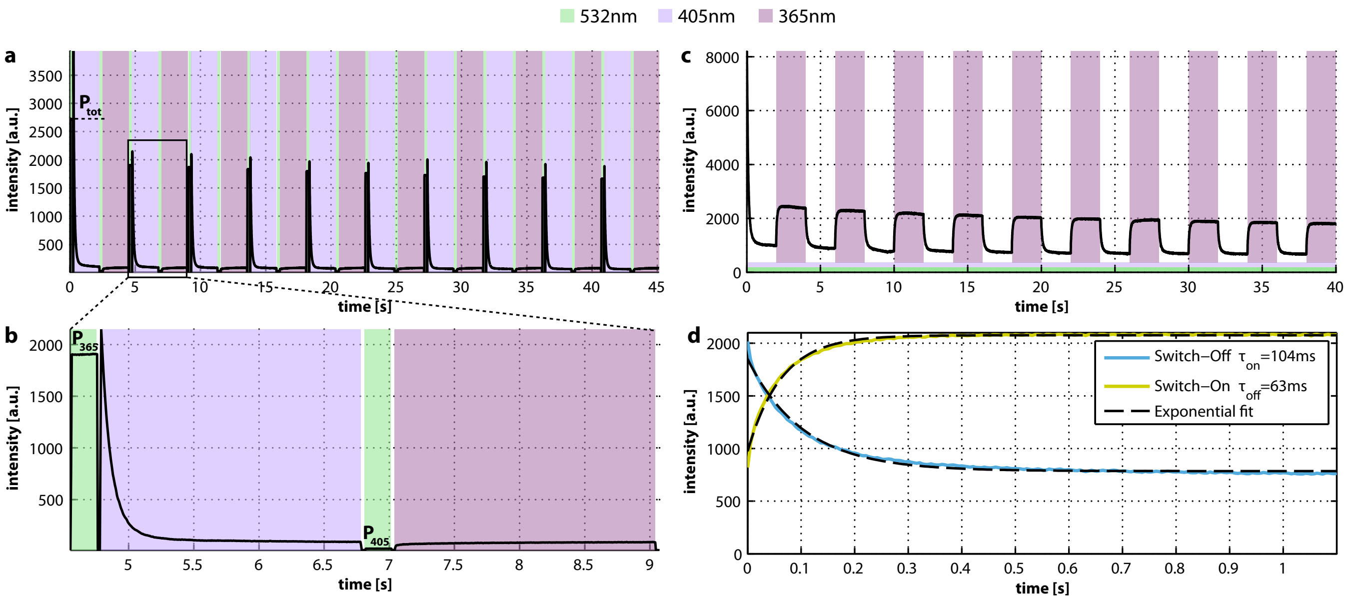

Supplementary Figure 4: Determination of Dreiklang switching kinetics. (a,b) Background-corrected fluorescence signal from a Dreiklang transfected Hela cell with alternated excitation of 532-405-532-365 nm light. The bleaching-corrected population levels P_{tot}, P_{365} and P_{405} allow the determination of the switching on-ratio for 365 nm and 405 nm light. (c,d) Fluorescence signal obtained with continuous 532 and 405 nm and pulsed 365 nm illumination. (d) shows the averaged switch-off and switch-on curves obtained from (c) with the corresponding exponential fits.

Supplementary Note 1: Multiplane SOFI analysis

Supplementary Figure 1 illustrates the five steps of the multiplane SOFI analysis:

Step 1: Raw cross-cumulation

Each registered pair of image sequences from consecutive depth channels was divided into 500-frame subsequences and processed with a 3D cross-cumulants analysis using voxel combinations without repetitions and zero time delays [1]. Supplementary Figure 2 gives an example of fourth-order voxel combinations. The frames of the upper plane were analyzed without preprocessing, whereas the frames of the lower plane were coregistered using an affine transformation (AT) and bilinear interpolation. The transformation parameters were obtained from a calibration measurement using fluorescent beads (beads centers were identified and co-registered using image segmentation and center-of-gravity computation). A subsequent fine-tuning of the image registration using a rigid transformation on the measurement data was necessary to correct for residual mechanical drift of the detection optics. From each bi-plane cross-cumulants analysis, only virtual planes and the untransformed upper physical plane were kept for further processing, because the interpolation of the lower depth plane introduces correlated noise in neighboring pixels. The bottommost plane (channel m) was analyzed with 2D cross-cumulants without preprocessing.

Step 2: Plane weight correction

The different detection responses in the channels were compensated by using a ratio histogram analysis of the two virtual planes obtained by a third order analysis. With an ideal 50:50 splitting, this ratio should be one because the distance factors are identical for the pixels in both virtual planes. The histogram is obtained by binning $\arctan(\text{plane}_{\text{III}}/\text{plane}_{\text{II}})$ and plotting it as a function of the ratio $\text{plane}_{\text{III}}/\text{plane}_{\text{II}}$. A Gaussian curve was fitted to the measured histogram and the center $1/\xi$ was used as a correction factor as indicated.

Step 3: Flatten cumulants

A distance factor that maximized the smoothness of the images was applied to correct for the different pixel weights in the raw cumulant images [2].

Alternative to steps 2 and 3: Standard deviation equalization

Instead of the above mentioned steps 2 and 3, a simplified and straightforward way to perform both plane-weight correction and flattening consists of dividing each cross-cumulant pixel group image by its respective standard deviation. We used that approach for Dreiklang data, where the third order cumulant images were too noisy to perform the ratio histogram analysis as described above.

Step 4: Transform cumulants

The bi-plane cumulant image blocks are transformed using the previously determined transformation masks in order to have all planes aligned.

Step 5: Balance cumulants

For Alexa 647 data, the cumulant responses were linearized by using a 3D Lucy-Richardson deconvolution with 50 iterations, taking the n-th root and reconvolving with an n-times size-reduced PSF [3]. The image shown is a third-order balanced SOFI image represented as a maximum intensity projection along the axial dimension with color-coding for the depth position. In the case of the much denser labelling by Dreiklang, we reduced the number of deconvolution steps to 5–10 and skipped the reconvolution step.

References

[1] Geissbuehler, S, Dellagiacoma, C. & Lasser, T. Comparison between SOFI and STORM. *Biomed. Opt. Express* **2,** 408–420 (2011).

[2] Dertinger, T, Colyer, R, Vogel, R, Enderlein, J. & Weiss, S. Achieving increased resolution and more pixels with superresolution optical fluctuation imaging (SOFI). *Opt. Express* **18,** 18875–18885 (2010).

[3] Geissbuehler, S. *et al.* Mapping molecular statistics with balanced super-resolution optical fluctuation imaging (bSOFI). *Opt. Nanoscopy* **1,** 4 (2012).